ACS APPLIED MATERIALS & INTERFACES

Research Article

www.acsami.org

PEDOT:PSS "Wires" Printed on Textile for Wearable Electronics

Yang Guo,[†] Michael T. Otley,[‡,∥] Mengfang Li,[†] Xiaozheng Zhang,[†] Sneh K. Sinha,[†] Gregory M. Treich,[†] and Gregory A. Sotzing*[,†,‡,§]

[†]Polymer Program, Institute of Materials Science, University of Connecticut, 97 North Eagleville Road, Storrs, Connecticut 06269, United States

[‡]Department of Chemistry, University of Connecticut, 55 North Eagleville Road, Storrs, Connecticut 06269, United States

[§]Department of Physics, University of Connecticut, 97 North Eagleville Road, Storrs, Connecticut 06269, United States

Supporting Information

ABSTRACT: Herein, the fabrication of all-organic conductive wires is demonstrated by utilizing patterning techniques such as inkjet printing and sponge stencil to apply poly(3,4-ethylenedioxythiophene) polystyrenesulfonate (PEDOT:PSS) onto nonwoven polyethylene terephthalate (PET) fabric. The coating of the conducting polymer is only present on the surface of the substrate (penetration depth ~ 200 μm) to retain the functionality and wearability of the textile. The wires fabricated by different patterning techniques provide a wide range of resistance, i.e., tens of kΩ/□ to less than 2 Ω/□ that allows the resistance to be tailored to a specific application. The sheet resistance is measured to be as low as 1.6 Ω/□, and the breakdown current is as high as 0.37 A for a 1 mm wide line. The specific breakdown current exceeds the previously reported values of macroscopic carbon nanotube based materials. Simple circuits composed of the printed wires are demonstrated, and resistance of the circuit from the measurement agrees with the calculated value based on Kirchhoff's rules. Additionally, the printed PEDOT:PSS wires show less than 6.2% change in sheet resistance after three washing and drying cycles using detergent.

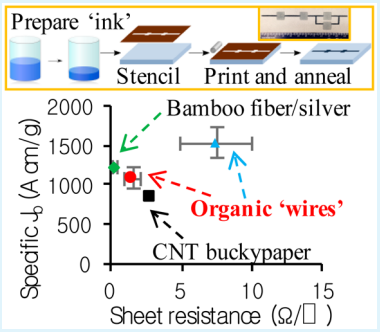

KEYWORDS: *electronic textile, wearable electronics, PEDOT:PSS, conducting polymer, patterning*

INTRODUCTION

Flexible/conformable and wearable electronics have shown tremendous potential in various fields including wireless communications,[1] thin film transistors,[2,3] displays,[4,5] chemical/biological sensors,[6−8] light-emitting electrochemical cells,[9] electronic skin,[10,11] and physiological/health monitors,[12,13] etc. These technologies are mainly based on flexible thin films or polymers incorporated with conducting materials such as metal nanoparticles/nanowires,[14] carbon nanotubes (CNTs),[6] graphene,[7] conducting polymers,[15] silicon-based semiconductors,[3] and indium tin oxide (ITO).[16] Organic conductors, especially electrically conducting polymers, present exceptional advantages, such as lightweight, low processing temperatures, low cost, good adhesion to flexible polymeric substrates, and compatibility with various processing techniques. The unique electrochemical properties of conducting polymers make them great candidates for the selective sensing layer.[17] Among them, polyaniline and polythiophene offer great advantages in terms of solubility and printability.[18] On the other hand, the conductivity of these polymers can be adjusted in a wide range by controlling doping levels.[19] Thus, conducting polymers have become promising candidates for flexible and wearable electronics with the advance in the stability of the material recently.

In particular, poly(3,4-ethylenedioxythiophene) (PEDOT) is able to form a stable particle suspension in water with polystyrenesulfonate (PSS) as a counterion and therefore has become the standard for conducting polymers being compatible with various open-air deposition methods.[20] The comfort and appearance are especially important for applications in wearable electronics. Conducting polymers offer a wide range of colors and, unlike metal, do not cause skin irritation and long-term toxicity under direct contact. PEDOT:PSS has been reported to have no cytotoxicity.[21] Scheme 1 shows the chemical structure of PEDOT:PSS consisting of the conjugated poly(3,4-ethylenedioxythiophene) and PSS to counterbalance the charge of

Scheme 1. Chemical Structure of PEDOT:PSS

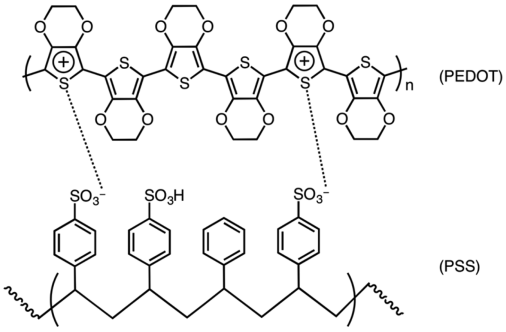

Received: July 3, 2016
Accepted: September 15, 2016

DOI: 10.1021/acsami.6b08036
ACS Appl. Mater. Interfaces XXXX, XXX, XXX−XXX

the charge carriers. The conductivity of the resulting film prepared from PEDOT:PSS aqueous suspension largely depends on the ratio of the two components. It has been reported that the addition of selected polar solvents as "secondary dopants", such as dimethyl sulfoxide (DMSO), sorbitol, diethylene glycol, and *N*-methylpyrrolidone (NMP) increases the conductivity of PEDOT:PSS films by 2−3 orders of magnitude.[22−25] While "primary dopants" neutralize the extra charges on conjugated polymers created through oxidizing or reducing during the doping process, secondary dopants are typically considered to expand the polymer chains as a result of the interaction between the dopants and the polymers and thus improve the conductivity.[26,27] Other methods to improve the conductivity of PEDOT:PSS film include post-treatment with acids, ethanol, geminal diol, and inorganic salts, etc.[28−30] Despite great efforts, the mechanism of conductivity enhancement is not completely clear. Experts suggested that both methods induce rearrangement in film morphology during drying to increase the phase separation of PEDOT and PSS.[31] This change leads to a better conducting network of PEDOT and, thus, an enhancement of electrical conductivity.

Electronic textiles (E-textiles) hold a sizable market of future wearable electronics as the high-throughput manufacturing in the fabric industry has been well established and the fiber-based structures of textiles provide deformable and breathable characteristics of clothing. However, combining electronic components with the highly porous, multiscale three-dimensional fiber structures is challenging. Current research is focused on incorporating metal containing materials, such as metal wires and metal particles, into textiles by sewing, braiding, weaving, knitting, coating/lamination, and printing, etc.[32] Such E-textiles often exhibit a metallic appearance and poor washing stability.[33] There is some work on patterning organic conductors PEDOT:PSS on flexible substrates such as polymer films and textiles using inkjet printing or screen printing to fabricate flexible electronics.[34−36] In spite of a few studies on E-textiles with all-organic components,[4,37] more research is needed. Presented herein is an efficient yet versatile method to prepare all-organic conductive wires on a textile surface that can be adjusted to obtain a range of resistance and is available to large-scale manufacturing. It was reported previously that the conductivity of PEDOT:PSS was enhanced significantly from the phase segregation induced by the surface chemistry of the textile.[38] Series and parallel circuits consisting of the printed wires are demonstrated, and their resistance from the measurement agrees with theoretical calculations.

EXPERIMENTAL SECTION

Patterning of PEDOT:PSS Conductive Wires. For the sponge stencil method, PEDOT:PSS aqueous solution (Clevios PH1000, Haraeus) was mixed with 5 wt % dimethyl sulfoxide (DMSO) followed by removal of 60% of the liquid by weight at 60 °C. The apparent shear viscosity of PEDOT:PSS solution was measured with an AR-G2 rheometer (TA Instruments). A stencil with the desired pattern was placed atop of a 2.5 cm × 2.5 cm PET nonwoven fabric. The concentrated PEDOT:PSS solution was applied on top of the stencil with a sponge. The PEDOT:PSS conductive wires coated PET fabrics were annealed at 110 °C in an oven for 1 h. The patterning and annealing processes were repeated up to 5 times for the lowest sheet resistance and higher current carrying capacity. For inkjet printing, a PEDOT:PSS aqueous solution (Sigma-Aldrich, 739316) formulated for inkjet printing was used. The conductive ink contains 0.8% PEDOT:PSS, 1−5% ethanol, and 5−10% diethylene glycol. The conductive wires were printed on the substrate using a FUJIFILM Dimatix Materials printer (DMP-2800) and annealed under the same condition.

Characterization of the Conductive Wires. The sheet resistance and breakdown current were measured using a four-line probe method reported in our previous work,[38,39] which include a current source Keithley 224 programmable current supply (I < 101.1 mA) or power supply 3630 (I < 10 A), a Keithley 2400 digital multimeter, and a four-line probe cell. All the measurements were conducted at room temperature. At leaset four to eight samples were measured to compute average and standard deviation values for each data point. PEDOT:PSS coating on the fibers was characterized from cross-section images obtained with field emission scanning electron microscopy (FESEM, JEOL JSM-6335F). The cross-section samples were cut with a razor blade while the fabrics were submerged in liquid nitrogen to minimize the distortion due to sample preparation. The structure and printing resolution were characterized from reflected light optical microscopy images (Nikon Metaphot metallurgical microscope) since the samples are opaque.

Circuit Fabrication and Characterization. Circuits constructed of resistors in parallel and series were printed on PET nonwoven fabric utilizing the same method as the wires. The circuit diagram is shown in Figure 1a, where R_c and R_d are in parallel and R_a and R_b are in series.

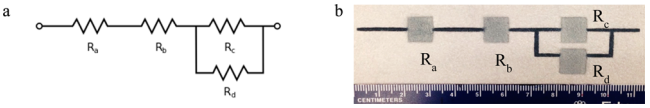

Figure 1. Demonstration of circuits printed with PEDOT:PSS. (a) Circuit diagram of resistors in series and parallel. (b) Image of the printed circuit constructed of resistors connected in a combination of series and parallel. R_a, R_b, R_c, and R_d are 1 cm × 1 cm squares representing resistors connected by 1 mm wide wires.

The resistors in both circuits are 1 cm × 1 cm squares printed from PEDOT:PSS aqueous solution with 5 wt % DMSO, and the connectors in the series circuit are 1 mm × 2 cm lines printed with the concentrated PEDOT:PSS solution following the same procedure of the wire fabrication. The resistances of each resistor, connector, and the whole circuit were measured with a Keithley 2420 SourceMeter.

Washing Durability Test. For samples without surface treatment, the printed PEDOT:PSS wires were soaked in DI water and soap water (1 wt %) under stirring (medium speed on a hot plate), respectively, followed by drying in the oven at 60 °C overnight. The soap water was prepared by mixing DI water with Tide Original Scent Liquid Laundry Detergent. The sheet resistance was measured before the initial washing and after each washing cycle via the four-line probe method. For the samples with hydrophobic treatment, Scotchgard Fabric & Upholstery Protector (3M) was sprayed on both sides evenly from a distance of 10−15 cm and the samples were allowed to dry at room temperature for 6 h before the washing experiments. Silver paste was applied at both ends of each wire to make connections to the source meter. The resistance of each sample was obtained from the I−V curve, and the sheet resistance was calculated based on the wire dimension. Six samples were measured to calculate the average values for each data point.

RESULTS AND DISCUSSION

Electrical Properties. Scheme 2 illustrates the fabrication of conductive PEDOT:PSS wires on polyethylene terephthalate (PET) nonwoven fabric using the sponge stencil method. The PEDOT:PSS aqueous solution was thickened by evaporating water in order to increase the viscosity of the "ink" and thus prevent bleeding on the porous structure of the textile. The apparent shear viscosity of the concentrated ink is 2 orders of magnitude higher at low shear rates. (Supporting Information Figure S1) Then a sponge applicator was used to transfer the "ink" atop the fabric surface covered by a stencil. In this study, a

DOI: 10.1021/acsami.6b08036
ACS Appl. Mater. Interfaces XXXX, XXX, XXX−XXX

Scheme 2. Fabrication Procedure of Patterning PEDOT:PSS on PET Nonwoven Fabric Using the Sponge Stencil Method

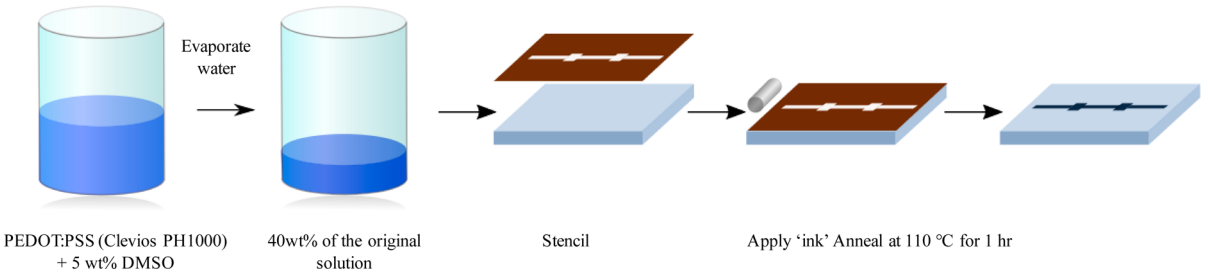

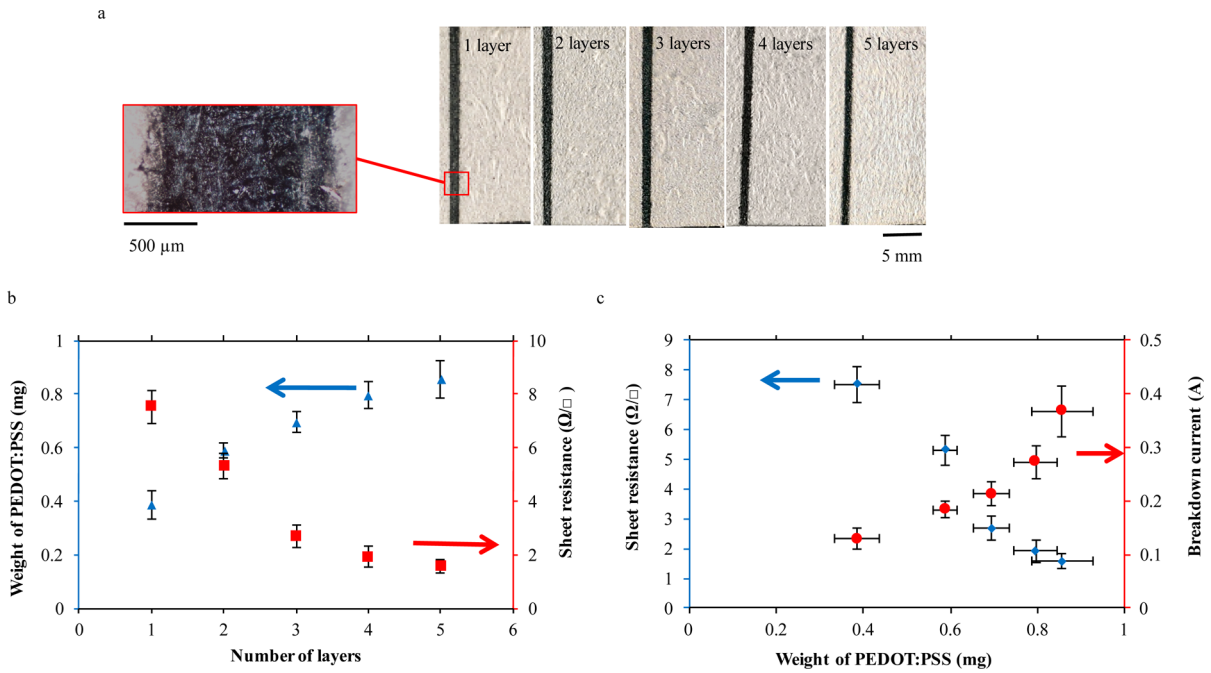

Figure 2. (a) Images of 1 mm conductive wires with one to five layers of coatings. The inserted image is a representative optical microscope image of a 1 mm wire. (b) Weight of PEDOT:PSS (blue triangles) and sheet resistance (red squares) of 1 mm wires as a function of the number of layers. (c) Improvement of electrical properties of conductive wires with the weight of PEDOT:PSS (blue diamonds indicate sheet resistance while red dots indicate breakdown current).

rectangular shape with the length of 2.5 cm and width of 1−5 mm was chosen to imitate wire structures.

Conductive wires fabricated from different patterning methods can have dissimilar electrical properties since the electrical properties significantly depend on the morphology of the conducting polymers. Inkjet printing, a noncontact technique, yields higher sheet resistance than stencil patterning methods. A 5 mm wide line with 10 layers of coating from inkjet printing contains 0.15 mg of PEDOT:PSS and shows a sheet resistance of 3185.7 Ω/□. The sheet resistance of wires with the same dimension fabricated from the sponge stenciling (1.59 mg of PEDOT:PSS) is 2.7 Ω/□, 3 orders of magnitude lower. Despite the versatility of pattern design and the high resolution (50−100 μm) of inkjet printing that benefits from the picoliter-sized droplets, only a small amount of the material is deposited on the surface each time. However, it can be resolved by industrial high-throughput inkjet printers. It is challenging to deposit a continuous film onto the rough surface of textiles now that the diameter of the fiber in the nonwoven PET is ca. 3 μm and the distance between fiber bundles can be 50 μm (Figure S2). Failure to make connections between fibers could lead to high resistance. In addition, the adhesion between layers of PEDOT:PSS depends on the spreading of the droplets for inkjet printing, whereas pressure is applied to the surface during stencil-based printing. The superior adhesion between different layers provides a better conducting network. Surface plasma treatment has been reported to tune the wettability of the substrates and thus the electrical properties of PEDOT:PSS printed tracks.[40] A wide range of resistances can be achieved by utilizing different depositing methods or tuning the formulation of the PEDOT:PSS suspension. Here the focus will be on the sponge stencil method.

To demonstrate the capability of conductive wires, lines with a different number of layers (1−5) and widths (1−5 mm) were patterned onto the fabric surface. Figure 2a shows images of 1 mm wires patterned using the sponge stencil method. The resolution of printed wires was obtained from optical microscope images as shown in the inserted image in Figure 1a. With the number of coating layers and line width increasing, the lines maintained sharp edges without bleeding. The penetration depth into the textile is another important dimension of the wires to determine the electrical properties. From the cross-section SEM images and reflected optical microscope images (Figure 3), it was observed that the penetration depth is less than 200 μm independent of the number of coating layers. This is because the individual fibers in

DOI: 10.1021/acsami.6b08036
ACS Appl. Mater. Interfaces XXXX, XXX, XXX−XXX

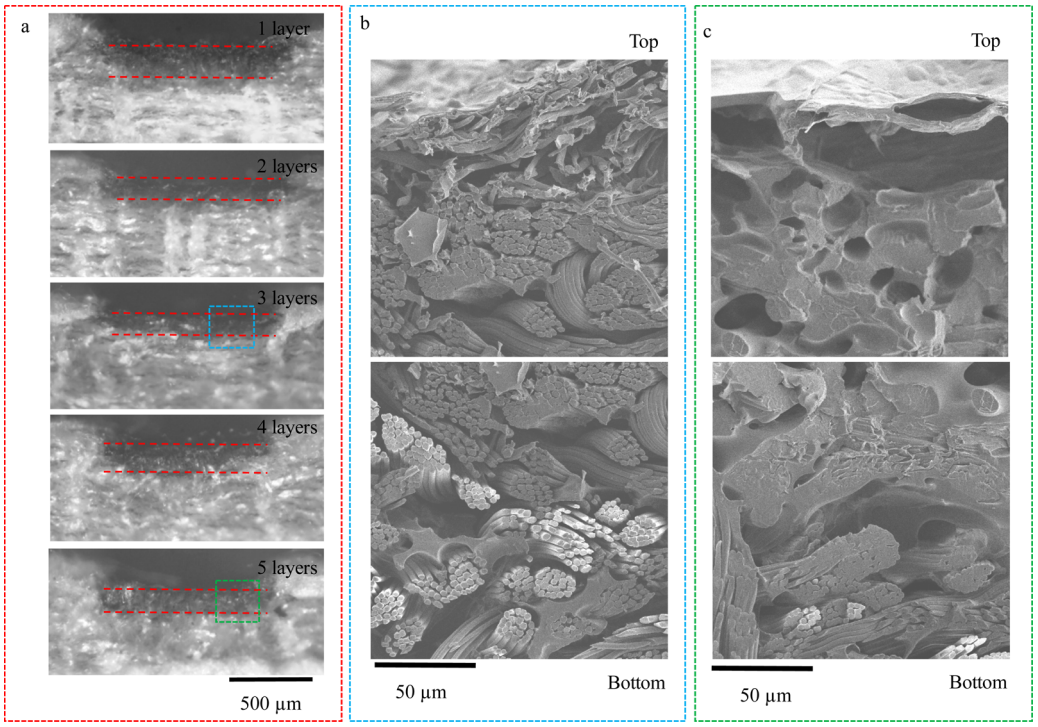

Figure 3. Cross-section of printed PEDOT:PSS wires fabricated using sponge stencil method. (a) Reflected microscope images of the cross sections of 1 mm wide wires with one to five layers of coatings, respectively. The red dashed lines indicate the surface of wires and the maximum penetration position. (b and c) Cross-section SEM images of wires with three and five layers of coatings, respectively.

the nonwoven fabric form a random and complex network which acts as a filter for the ink. After the first printing layer, the coating of the conducting polymers limits further penetration into the textile in the following cycles. The average penetration depths obtained from reflected optical microscope images are summarized in Table 1. The average penetration depths are approximately the same within experimental errors for samples with one to three layers of coatings. It rises to 154 ± 12 μm with four layers and does not further increase with another layer of coating. The weight of the fabric was measured both before and after the coating to determine the mass of the conductor.

Table 1. Average Penetration Depth of 1 mm Wide PEDOT:PSS Wires Printed with Sponge Stencil Method Obtained from Reflective Optical Microscope

no. of layers	av penetration depth (μm)
1	111 ± 12
2	94 ± 14
3	102 ± 20
4	154 ± 12
5	156 ± 16

Conductive wires exhibit Ohmic behavior until they reach the breakdown current. The weight of the conductor increases with the number of layers patterned on the surface but changes are much slower as the fabric is saturated (Figure 2b). The corresponding sheet resistance of the conductive wires decreases from 7.5 to 1.6 Ω/□ as more layers of PEDOT:PSS are patterned (Figure 2b). The electrical properties of 1 mm conductive wires are summarized in Figure 2c based on the weight of conductors. The sheet resistance decreases linearly as a function of PEDOT:PSS weight while the breakdown current rises from 0.13 to 0.37 A DC.

The electrical properties of the conductive wires are further investigated in terms of the line width. Figure 4a shows representative images of conductive wires with widths of 1, 3, and 5 mm, respectively. The conductive coating shows great homogeneity on the textile for different line widths, which is essential to limit variations in resistance through the area and thus present local heating due to higher resistance. The weight of PEDOT:PSS increases linearly as a function of the width of the line (as shown in Figure 4b) that further indicates a uniform coating. The wires with a width of 1−5 mm have a similar sheet resistance (2.2 Ω/□ as the lowest and 3.1 Ω/□ as the highest). Figure 4c compares the electrical properties with respect to the weight of the conductor. It shows that the sheet resistance is similar because the amount of conductor per surface area is approximately the same, whereas the breakdown current increases linearly from 0.29 to 0.90 A DC as a result of the weight of PEDOT.

So far, it has been demonstrated that the printed wires are capable of carrying DC current sufficiently for small-signal electronics (milliamps) with less than 1 mg of organic conductor within a dimension of 1 mm × 25 mm × 0.2 mm. Some applications including cables and electronic interconnections require the conductor to operate under high current. Organic conductors with extraordinary specific electrical properties (normalized by density) are promising candidates to replace metals especially for such applications in need of lightweight. The current carrying capacity (CCC), or normally known as ampacity, is the maximum current a cable can carry without inducing short- or long-term damage to both the conductor and the insulating materials.[41] The CCC of individual carbon nanotubes (CNTs) was reported to exceed 10^9 A/cm^2,[42,43] higher than the theoretical electromigration

DOI: 10.1021/acsami.6b08036
ACS Appl. Mater. Interfaces XXXX, XXX, XXX−XXX

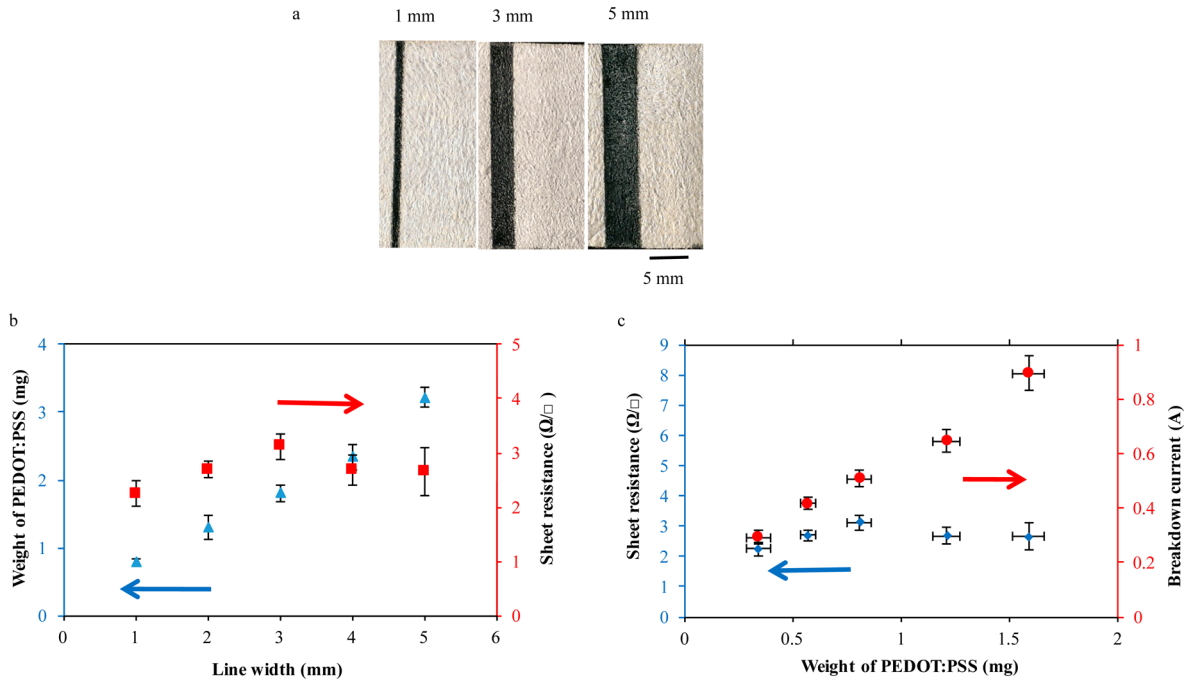

Figure 4. (a) Images of 1, 3, and 5 mm conductive wires with five layers of coatings. (b) Weight of PEDOT:PSS (blue triangles) and sheet resistance (red squares) of conductive wires with five layers of coatings as a function of the line width, respectively. (c) Improvement of electrical properties of conductive wires with the weight of PEDOT:PSS (blue diamonds indicate sheet resistance while red dots indicate breakdown current).

limit of copper, 10^6 A/cm^2.[44] However, when CNTs form macroscopic structures such as fibers, films, or bundles, the resistivity increases dramatically due to intertube transport, thus resulting in significant Joule heating under high current density.[45] The CCC of macroscopic CNT-based materials is dependent on the volume-to-surface ratio, which influences the balance between Joule heating and thermal convection to the ambient. Therefore, the results from millimeter-sized CNT-based buckypapers measured under air were chosen to compare with this work.

Here, the specific current densities at breakdown of the printed PEDOT:PSS conductive wires are compared with PET fully infused with PEDOT:PSS, commercially available conductive textile containing metal, i.e., bamboo fiber with silver thread, as well as millimeter-sized CNT-based buckypapers. The PET fully infused with PEDOT:PSS and bamboo fiber/silver were cut into 1 mm × 2.5 cm strips for the measurement, whereas the CCC value of aligned single-walled CNT buckypaper was from the literature.[46] The results are presented in Figure 5, where the specific breakdown current densities of various conductors are plotted as a function of the sheet resistance. The printed PEDOT:PSS conductive wires show comparable or lower sheet resistance than CNT-based buckypapers and higher than bamboo fiber/silver. Similar breakdown currents were observed from the printed wires and fully infused fabrics indicating that the printing process does not influence the capacity of carrying current. The CCC values of the printed wires are comparable with that of bamboo fiber/silver. Interestingly, the specific breakdown currents of printed wires are higher than that of the macroscopic CNT-based buckypapers.

Printed Circuit. As mentioned above, the resistance of printed wires can be adjusted by using different patterning techniques or controlling the concentration of PEDOT:PSS solution and the amount of conductor applied to the fabric.

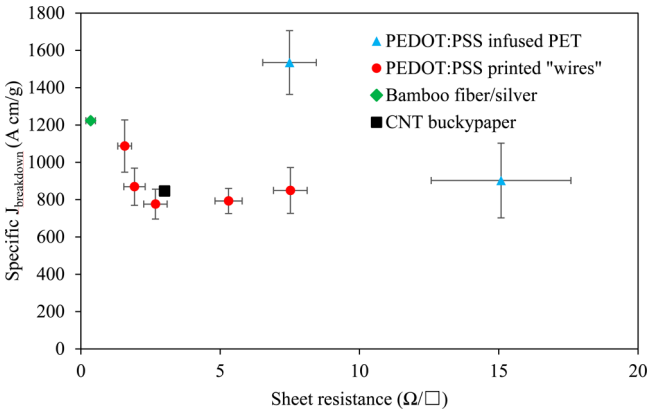

Figure 5. Comparison of specific breakdown current density of PET infused with PEDOT:PSS (blue triangle), printed PEDOT:PSS conductive wires (red dot), aligned CNT buckypaper from literature (black square), and bamboo fiber/silver (green diamond) normalized by the density of the conductor.

Printed wires with low resistance serve as the "connection" of other components whereas those with high resistance work as the resistor in a circuit. Figure 1 illustrated a circuit composed of printed wires that function as both the resistor and the conductive connections between different resistors. R_a and R_b are connected in series with the parallel combination of R_c and R_d as shown in the circuit diagram (Figure 1a). The resistance of each element as well as the total resistance of the circuit were measured, and the values and experimental errors of three printed circuits are listed in Table 2. The resistance of circuit 1 calculated according to Kirchhoff's rules is shown in eqs 1 and 2 as an example. The total resistance of the circuit is measured to be 3859 Ω which agrees with the calculation (3783 Ω) despite a small difference due to contact resistance between the circuit and the source meter.

DOI: 10.1021/acsami.6b08036
ACS Appl. Mater. Interfaces XXXX, XXX, XXX−XXX

Table 2. Resistance Values of Printed Circuits

sample no.	R_a (Ω)	R_b (Ω)	R_c (Ω)	R_d (Ω)	R_{total} (Ω) measd	R_{total} (Ω) calcd	exptl error (%)
1	1361	1841	4152	675	3859	3783	2.0
2	608	739	615	967	1723	1622	5.9
3	534	378	453	129	1012	1125	10.0

$$\frac{1}{R_{parallel}} = \frac{1}{R_c} + \frac{1}{R_d}, \quad R_{parallel} = 581\ \Omega \tag{1}$$

$$R_{total} = R_{series} = R_a + R_b + R_{parallel} = 3783\ \Omega \tag{2}$$

Washing Stability. The ability to sustain the electrical properties under sweat and washing while maintaining the feel of a fabric is essential for modern wearable electronics. The washing stability of the printed wires has been investigated by monitoring the change in sheet resistance after each washing and drying cycle. R_{s0} and R_{sN} are the sheet resistance values before the washing test and after the Nth washing and drying cycle, respectively. The relative change in sheet resistance is calculated from

$$\text{relative } \Delta R_s/\% = \frac{R_{sN} - R_{s0}}{R_{s0}} \times 100 \tag{3}$$

Four different washing conditions were explored in this study including washing in deionized (DI) water with and without hydrophobic surface treatment and washing in soap water with and without hydrophobic treatment. The concentration of the soap water (1 wt %) used in this study is approximately 10 times of that in a typical washing machine (0.06−0.17 wt %).[47] The wires were dried for an exceeding amount of time (12 h) at 60 °C which is higher than the temperature in a dryer under the high mode (~57 °C). The relative change in sheet resistance is plotted after each washing/drying cycle for all the conditions in Figure 6, and details are listed in Table S1 and Table S2. A significant increase in sheet resistance is observed for both DI water (26% after three cycles) and soap water washing (106% after three cycles). The sheet resistance continues to increase after each washing and drying cycle for samples without hydrophobic treatment. However, the printed wires indicate pronounced improvement in washing stability after a hydrophobic treatment. Specifically, the relative increase of sheet resistance is below 6.2% for soap water washing after 3 washing and drying cycles with no trend of further changes.

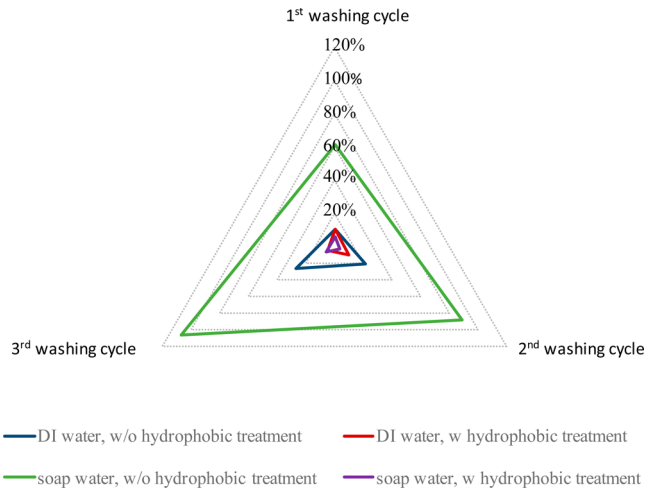

Figure 6. Relative increase in sheet resistance $(R_{sN} - R_{s0})/R_{s0} \times 100\%$ of 1 mm wide printed PEDOT:PSS wires after each washing and drying cycle. The blue and green lines represent the average results of six samples without hydrophobic treatment in DI water and soap water, respectively, while the red and purple lines are the average results of six samples with hydrophobic treatment in DI water and soap water, respectively, under the same washing and drying conditions.

CONCLUSION

All-organic conductive wires were fabricated using scalable patterning techniques such as sponge stencil and inkjet printing using the conducting polymer PEDOT:PSS. The current carrying capacity, CCC, of the printed wires is approximately 10^3 A/cm^2, making these conductive lines on textile suitable for many different applications in wearable electronics. The specific breakdown current density of the printed wires exceeds the value of CNT-based buckypaper having comparable dimension and is competitive with some commercially available silver containing conductive fabrics. Series and parallel circuits composed of the organic wires are demonstrated, and the resistances of the circuits are in good agreement with calculation. As a measure for preliminary durability of these fabrics, PEDOT:PSS conductive wires on polyethylene terephthalate textile retained its electronic functionality after three wash/dry cycles with the fabric having a hydrophobic surface treatment.

ASSOCIATED CONTENT

Supporting Information

The Supporting Information is available free of charge on the ACS Publications website at DOI: 10.1021/acsami.6b08036.

Viscosities of PEDOT:PSS solution (clevios PH1000 with 5 wt % DMSO) before and after removal of 60 wt % of liquid, a SEM image of the cross-section of PET nonwoven textiles, estimation of CCC values, and washing stability data of printed wires (PDF)

AUTHOR INFORMATION

Corresponding Author

*E-mail: g.sotzing@uconn.edu.

Present Address

‖M.T.O. is currently at Northwestern University, Evanston, IL 60208.

Notes

The authors declare no competing financial interest.

ACKNOWLEDGMENTS

We thank Technology Commercialization Partner of the University of Connecticut for the Prototype Grant.

REFERENCES

(1) Russo, A.; Ahn, B. Y.; Adams, J. J.; Duoss, E. B.; Bernhard, J. T.; Lewis, J. A. Pen-on-Paper Flexible Electronics. *Adv. Mater.* **2011**, *23* (30), 3426−3430.

(2) Vosgueritchian, M.; Lipomi, D. J.; Bao, Z. Highly Conductive and Transparent PEDOT:PSS Films with a Fluorosurfactant for Stretchable and Flexible Transparent Electrodes. *Adv. Funct. Mater.* **2012**, *22* (2), 421−428.

(3) Sun, Y.; Rogers, J. A. Inorganic Semiconductors for Flexible Electronics. *Adv. Mater.* **2007**, *19* (15), 1897−1916.

DOI: 10.1021/acsami.6b08036
ACS Appl. Mater. Interfaces XXXX, XXX, XXX−XXX

(4) Ding, Y.; Invernale, M. A.; Sotzing, G. A. Conductivity Trends of Pedot-Pss Impregnated Fabric and the Effect of Conductivity on Electrochromic Textile. *ACS Appl. Mater. Interfaces* **2010**, *2* (6), 1588−1593.
(5) Matyba, P.; Yamaguchi, H.; Chhowalla, M.; Robinson, N. D.; Edman, L. Flexible and Metal-Free Light-Emitting Electrochemical Cells Based on Graphene and PEDOT-PSS as the Electrode Materials. *ACS Nano* **2011**, *5* (1), 574−580.
(6) Jeon, J.-Y.; Ha, T.-J. Waterproof Electronic-Bandage with Tunable Sensitivity for Wearable Strain Sensors. *ACS Appl. Mater. Interfaces* **2016**, *8*, 2866−2871.
(7) Tang, Y.; Zhao, Z.; Hu, H.; Liu, Y.; Wang, X.; Zhou, S.; Qiu, J. Highly Stretchable and Ultrasensitive Strain Sensor Based on Reduced Graphene Oxide Microtubes-Elastomer Composite. *ACS Appl. Mater. Interfaces* **2015**, *7* (49), 27432−27439.
(8) Saravanakumar, B.; Soyoon, S.; Kim, S. Self-Powered pH Sensor Based on a Flexible Organic − Inorganic Hybrid Composite Nanogenerator. *ACS Appl. Mater. Interfaces* **2014**, *6* (16), 13716−13723.
(9) Zhang, S.; Hubis, E.; Girard, C.; Kumar, P.; DeFranco, J.; Cicoira, F. Water Stability and Orthogonal Patterning of Flexible Micro-Electrochemical Transistors on Plastic. *J. Mater. Chem. C* **2016**, *4* (7), 1382−1385.
(10) Kim, D.-H.; Lu, N.; Ma, R.; Kim, Y.-S.; Kim, R.-H.; Wang, S.; Wu, J.; Won, S. M.; Tao, H.; Islam, A.; Yu, K. J.; Kim, T. -i.; Chowdhury, R.; Ying, M.; Xu, L.; Li, M.; Chung, H.-J.; Keum, H.; McCormick, M.; Liu, P.; Zhang, Y.-W.; Omenetto, F. G.; Huang, Y.; Coleman, T.; Rogers, J. A. Epidermal Electronics. *Science (Washington, DC, U. S.)* **2011**, *333* (6044), 838−843.
(11) Mannsfeld, S. C. B.; Tee, B. C.-K.; Stoltenberg, R. M.; Chen, C. V. H.-H.; Barman, S.; Muir, B. V. O.; Sokolov, A. N.; Reese, C.; Bao, Z. Highly Sensitive Flexible Pressure Sensors with Microstructured Rubber Dielectric Layers. *Nat. Mater.* **2010**, *9* (10), 859−864.
(12) Wang, X.; Gu, Y.; Xiong, Z.; Cui, Z.; Zhang, T. Silk-Molded Flexible, Ultrasensitive, and Highly Stable Electronic Skin for Monitoring Human Physiological Signals. *Adv. Mater.* **2014**, *26* (9), 1336−1342.
(13) Scalisi, R. G.; Paleari, M.; Favetto, A.; Stoppa, M.; Ariano, P.; Pandolfi, P.; Chiolerio, A. Inkjet Printed Flexible Electrodes for Surface Electromyography. Org. Electron. physics. *Org. Electron.* **2015**, *18*, 89−94.
(14) Rida, A.; Yang, L.; Vyas, R.; Tentzeris, M. M. Conductive Inkjet-Printed Antennas on Flexible Low-Cost Paper-Based Substrates for RFID and WSN Applications. *IEEE Antennas Propag. Mag.* **2009**, *51*, 13−23.
(15) Kim, N.; Kang, H.; Lee, J. H.; Kee, S.; Lee, S. H.; Lee, K. Highly Conductive All-Plastic Electrodes Fabricated Using a Novel Chemically Controlled Transfer-Printing Method. *Adv. Mater.* **2015**, *27* (14), 2317−2323.
(16) Ellmer, K. Past Achievements and Future Challenges in the Development of Optically Transparent Electrodes. *Nat. Photonics* **2012**, *6* (12), 809−817.
(17) Janata, J.; Josowicz, M. Conducting Polymers in Electronic Chemical Sensors. *Nat. Mater.* **2003**, *2* (1), 19−24.
(18) Bocchini, S.; Chiolerio, A.; Porro, S.; Accardo, D.; Garino, N.; Bejtka, K.; Perrone, D.; Pirri, C. F. Synthesis of Polyaniline-Based Inks, Doping Thereof and Test Device Printing towards Electronic Applications. *J. Mater. Chem. C* **2013**, *1* (33), 5101−5109.
(19) MacDiarmid, A. G. Synthetic Metals": A Novel Role for Organic Polymers (Nobel Lecture). *Angew. Chem., Int. Ed.* **2001**, *40* (14), 2581−2590.
(20) Groenendaal, L.; Jonas, F.; Freitag, D.; Pielartzik, H.; Reynolds, J. R. Poly(3,4-Ethylenedioxythiophene) and Its Derivatives: Past, Present, and Future. *Adv. Mater.* **2000**, *12* (7), 481−494.
(21) Miriani, R. M.; Abidian, M. R.; Kipke, D. R. Cytotoxic Analysis of the Conducting Polymer PEDOT Using Myocytes. *30th Annual International Conference of the IEEE Engineering in Medicine and Biology Society*; IEEE: New York, 2008; Vol. *2008*, pp 1841−1844, DOI: 10.1109/IEMBS.2008.4649538.
(22) Kim, J. Y.; Jung, J. H.; Lee, D. E.; Joo, J. Enhancement of Electrical Conductivity of poly(3,4-ethylenedioxythiophene)/poly(4-Styrenesulfonate) by a Change of Solvents. *Synth. Met.* **2002**, *126* (2−3), 311−316.
(23) Huang, J.; Miller, P. F.; Wilson, J. S.; De Mello, A. J.; De Mello, J. C.; Bradley, D. D. C. Investigation of the Effects of Doping and Post-Deposition Treatments on the Conductivity, Morphology, and Work Function of poly(3,4- Ethylenedioxythiophene)/poly(styrene Sulfonate) Films. *Adv. Funct. Mater.* **2005**, *15* (2), 290−296.
(24) Ouyang, J.; Xu, Q.; Chu, C. W.; Yang, Y.; Li, G.; Shinar, J. On the Mechanism of Conductivity Enhancement in poly(3,4-Ethylenedioxythiophene):poly(styrene Sulfonate) Film through Solvent Treatment. *Polymer* **2004**, *45* (25), 8443−8450.
(25) Ouyang, J.; Chu, C. W.; Chen, F. C.; Xu, Q.; Yang, Y. High-Conductivity poly(3,4-Ethylenedioxythiophene):poly(styrene Sulfonate) Film and Its Application in Polymer Optoelectronic Devices. *Adv. Funct. Mater.* **2005**, *15* (2), 203−208.
(26) Chiolerio, A.; Bocchini, S.; Scaravaggi, F.; Porro, S.; Perrone, D.; Beretta, D.; Caironi, M.; Fabrizio Pirri, C. Synthesis of Polyaniline-Based Inks for Inkjet Printed Devices: Electrical Characterization Highlighting the Effect of Primary and Secondary Doping. *Semicond. Sci. Technol.* **2015**, *30* (10), 104001.
(27) Kar, P. *Doping in Conjugated Polymers*; John Wiley & Sons: Hoboken, NJ, USA, 2013.
(28) Xia, Y.; Sun, K.; Ouyang, J. Solution-Processed Metallic Conducting Polymer Films as Transparent Electrode of Optoelectronic Devices. *Adv. Mater.* **2012**, *24* (18), 2436−2440.
(29) Xia, Y.; Zhang, H.; Ouyang, J. Highly Conductive PEDOT:PSS Films Prepared through a Treatment with Zwitterions and Their Application in Polymer Photovoltaic Cells. *J. Mater. Chem.* **2010**, *20* (43), 9740.
(30) Xia, Y.; Ouyang, J. Salt-Induced Charge Screening and Significant Conductivity Enhancement of Conducting poly(3,4-Ethylenedioxythiophene): Poly(styrenesulfonate). *Macromolecules* **2009**, *42* (12), 4141−4147.
(31) Greczynski, G.; Kugler, T.; Salaneck, W. R. Characterization of the PEDOT-PSS System by Means of X-Ray and Ultraviolet Photoelectron Spectroscopy. *Thin Solid Films* **1999**, *354* (1), 129−135.
(32) Stoppa, M.; Chiolerio, A. Wearable Electronics and Smart Textiles: A Critical Review. *Sensors* **2014**, *14* (7), 11957−11992.
(33) Liu, H.; Lv, M.; Deng, B.; Li, J.; Yu, M.; Huang, Q.; Fan, C. Laundering Durable Antibacterial Cotton Fabrics Grafted with Pomegranate-Shaped Polymer Wrapped in Silver Nanoparticle Aggregations. *Sci. Rep.* **2014**, *4*, 5920.
(34) Hu, B.; Li, D.; Ala, O.; Manandhar, P.; Fan, Q.; Kasilingam, D.; Calvert, P. D. Textile-Based Flexible Electroluminescent Devices. *Adv. Funct. Mater.* **2011**, *21* (2), 305−311.
(35) Takamatsu, S.; Lonjaret, T.; Crisp, D.; Badier, J.-M.; Malliaras, G. G.; Ismailova, E. Direct Patterning of Organic Conductors on Knitted Textiles for Long-Term Electrocardiography. *Sci. Rep.* **2015**, *5*, 15003.
(36) Sirringhaus, H.; Kawase, T.; Friend, R. H.; Shimoda, T.; Inbasekaran, M.; Wu, W.; Woo, E. P. High-Resolution Inkjet Printing of All-Polymer Transistor Circuits. *Science (Washington, DC, U. S.)* **2000**, *290* (5499), 2123−2126.
(37) Seyedin, M. Z.; Razal, J. M.; Innis, P. C.; Wallace, G. G. Strain-Responsive polyurethane/PEDOT:PSS Elastomeric Composite Fibers with High Electrical Conductivity. *Adv. Funct. Mater.* **2014**, *24* (20), 2957−2966.
(38) Sotzing, G. A. Electrically Conductive Synthetic Fiber and Fibrous Substrate, Method of Making, and Use Thereof. 20150017421, 2015.
(39) Hiremath, R. K.; Rabinal, M. K.; Mulimani, B. G. Simple Setup to Measure Electrical Properties of Polymeric Films. *Rev. Sci. Instrum.* **2006**, *77* (12), 126106.
(40) Chiolerio, A.; Rivolo, P.; Porro, S.; Stassi, S.; Ricciardi, S.; Mandracci, P.; Canavese, G.; Bejtka, K.; Pirri, C. F. Inkjet-Printed PEDOT:PSS Electrodes on Plasma-Modified PDMS Nanocomposites:

DOI: 10.1021/acsami.6b08036
ACS Appl. Mater. Interfaces XXXX, XXX, XXX−XXX

Quantifying Plasma Treatment Hardness. *RSC Adv.* **2014**, *4* (93), 51477−51485.
(41) Waghorne, J. H.; Ogorodnikov, V. E. Current Carrying Capacity of ACSR Conductors. *Trans. Am. Inst. Electr. Eng.* **1951**, *70*, 1159−1162.
(42) Wei, B. Q.; Vajtai, R.; Ajayan, P. M. Reliability and Current Carrying Capacity of Carbon Nanotubes. *Appl. Phys. Lett.* **2001**, *79* (8), 1172−1174.
(43) Collins, P. G.; Hersam, M.; Arnold, M.; Martel, R.; Avouris, P. Current Saturation and Electrical Breakdown in Multiwalled Carbon Nanotubes. *Phys. Rev. Lett.* **2001**, *86* (14), 3128−3131.
(44) Hauder, M.; Gstöttner, J.; Hansch, W.; Schmitt-Landsiedel, D. Scaling Properties and Electromigration Resistance of Sputtered Ag Metallization Lines. *Appl. Phys. Lett.* **2001**, *78* (6), 838.
(45) Wang, X.; Behabtu, N.; Young, C. C.; Tsentalovich, D. E.; Pasquali, M.; Kono, J. High-Ampacity Power Cables of Tightly-Packed and Aligned Carbon Nanotubes. *Adv. Funct. Mater.* **2014**, *24* (21), 3241−3249.
(46) Park, J. G.; Li, S.; Liang, R.; Fan, X.; Zhang, C.; Wang, B. The High Current-Carrying Capacity of Various Carbon Nanotube-Based Buckypapers. *Nanotechnology* **2008**, *19* (18), 185710.
(47) Zoller, U. *Handbook of Detergents, Part E: Applications*; CRC Press: Boca Raton, FL, USA, 2009

DOI: 10.1021/acsami.6b08036
ACS Appl. Mater. Interfaces XXXX, XXX, XXX−XXX